The SGLT2i Dapagliflozin Reduces RV Hypertrophy Independent of Changes in RV Pressure Induced by Pulmonary Artery Banding

Kim Connelly (connellyk@smh.ca)
St Michaels Hospital https://orcid.org/0000-0002-1031-3137
Ellen Wu
St Michael's Hospital Keenan Research Centre for Biomedical Science
Aylin Visram
St Michael's Hospital Keenan Research Centre for Biomedical Science
Mark K. Friedberg
Hospital for Sick Children Research Institute: SickKids Research Institute
Sri Nagarjun Batchu
St Michael's Hospital Keenan Research Centre for Biomedical Science
Veera Ganesh Yeera
St Michael's Hospital Keenan Research Centre for Biomedical Science
Kerri Thai
St Michael's Hospital Keenan Research Centre for Biomedical Science
Linda Nghiem
St Michael's Hospital Keenan Research Centre for Biomedical Science
Yanling Zhang
St Michael's Hospital Keenan Research Centre for Biomedical Science
Golam Kabir
St Michael's Hospital Keenan Research Centre for Biomedical Science
JF Desjardins
St Michael's Hospital Keenan Research Centre for Biomedical Science
Andrew Advani
St Michael's Hospital Keenan Research Centre for Biomedical Science
Richard E Gilbert
St Michael's Hospital Keenan Research Centre for Biomedical Science

Research Article

Keywords: RV pressure load; Extracellular water, SGLT2i, calcium handling

Posted Date: December 23rd, 2021

DOI: https://doi.org/10.21203/rs.3.rs-966875/v2

Abstract

Background— Sodium glucose linked transporter 2 (SGLT2) inhibition not only reduces morbidity and mortality in patients with diagnosed heart failure but also prevents the development of heart failure hospitalization in those at risk. While studies to date have focused on the role of SGLT2 inhibition in left ventricular failure, whether this drug class might be similarly efficacious in the treatment and prevention of right heart failure has not been unexplored.

Hypothesis: We hypothesized that SGLT2 inhibition would reduce the structural, functional and molecular responses to pressure overload of the right ventricle.

Methods: Thirteen-week-old Fischer F344 rats underwent pulmonary artery banding (PAB) or sham surgery prior to being randomized to receive either the SGLT2 inhibitor: dapagliflozin (0.5mg/kg/day) or vehicle by oral gavage. After six weeks of treatment, animals underwent transthoracic echocardiography and invasive hemodynamic studies. Animals were then terminated, and their hearts harvested for structural and molecular analyses.

Results: PAB induced features consistent with a compensatory response to increased right ventricular (RV) afterload with elevated mass, end systolic pressure, collagen content and alteration in calcium handling protein expression (all $p<0.05$ when compared to sham + vehicle). Dapagliflozin reduced RV mass, including both wet and dry weight as well as normalizing the protein expression of SERCA 2A, AMPkinase and LC3I/II ratio expression (all $p<0.05$).

Significance: Dapagliflozin reduces the structural, functional, and molecular manifestations of right ventricular pressure overload. Whether amelioration of these early changes in the RV may ultimately lead to a reduction in RV failure remains to be determined.

Introduction

Cardiovascular disease remains the number one cause of mortality in the developed world. It is now well established that right ventricular (RV) failure (RVF) is the most important determinant of mortality in diseases that directly stress the RV such as pulmonary hypertension (PH)[1,2]. The importance of RVF in populations such as adults with congenital heart disease make this a pressing problem[3]. Moreover, there is accumulating evidence that RVF in diverse cardiac diseases, including left ventricular failure (LVF), is a key determinant of morbidity and mortality[4]. Therefore, RV dysfunction and failure are important in every cardiovascular condition. Following a pathological stimulus (e.g., PH) the RV undergoes a response known as pathological remodeling[5,6]. Regardless of the etiology, key histopathological features of pathological RV remodeling include the development of RV hypertrophy (RVH), ventricular dilatation and excessive extracellular matrix (ECM) deposition (fibrosis)[7]. Whilst these changes are aimed at maintaining cardiac output and stabilizing the RV in the short-term, the long-term consequence is an inexorable progression to RVF and morbidity[8–10].

Despite advances in treatments in recent years, RVF secondary to PH remains a persistent and important clinical issue. Furthermore, treatment efforts to treat RVF have largely failed. Pharmacological strategies aimed at reducing pathological ventricular remodeling, via inhibition of “neuro-hormonal activity” i.e., sympathetic and renin-angiotensin-aldosterone activation, are minimally effective in the RV and consequently RVF overall[11–13]. As a result, novel mechanisms of RV remodeling must be uncovered to develop new therapies so that mortality/morbidity can be reduced.

The SGLT2i dapagliflozin has been shown to prevent hospitalization for heart failure in persons with type 2 DM both with and without atherosclerotic cardiovascular disease[14], and in persons with heart failure and reduced ejection fraction, dapagliflozin has been shown to reduce CV and all cause mortality, irrespective of diabetes status on top of guideline directed therapies[15]. The mechanisms of CV protection remain unclear but are likely to result from changes in preload, afterload, metabolism, renal function and direct cardiac effects[16–18]

Herein, we hypothesized that by inducing an osmotic diuresis (and possibly other cardio-protective mechanisms), dapagliflozin will reduce right ventricle (RV) pressure thereby leading to a reduction in right ventricular hypertrophy and reduce the propensity towards RVF. We chose to study the impact on RV hypertrophy by utilising the pulmonary artery banding model, as this model demonstrates features of RV pressure loading[19]

Materials And Methods

In vivo experiments

Animal study approval was obtained from St. Michael’s Hospital Animal Care Committee in accordance with the National Institute of Health’s Guide for the Care and Use of Laboratory Animals (NIH Publication No. 85-23, revised 1996).

Pulmonary artery banding model

Male Fischer F344 rats (200 g body weight) were randomized to either sham surgery (control) or RV pressure-load via pulmonary artery banding (PAB). Anesthesia was induced with Isoflurane (2-2.5% mixed with 1 L/min 100% O_2). After intubation, animals were mechanically ventilated using a volume-controlled respirator and oxygen-enriched room air. Positive end-expiratory pressure was maintained at 4 cmH_2O. Through a left thoracotomy the pulmonary artery (PA) was carefully dissected from the aorta. A silk thread was positioned under the PA and an 18-gauge needle placed alongside the PA. A suture was tied tightly around the needle, and the needle removed to produce a fixed PA constriction proportional to the needle diameter. The thorax was then closed in layers, and subcutaneous buprenorphine (15µg/kg) administered for postoperative pain relief. The combination of fixed PAB and animal growth resulted in progressive increase in RV pressure-load. Sham controls underwent the same procedure except for PAB. There were two separate groups of animals studied: Study 1 underwent assessment as described below. Briefly, animals were randomized to either vehicle, or dapagliflozin -given 0.5mg/kg BID by oral gavage.

Animals were then followed for 6 weeks, at which time they underwent repeat echocardiography, invasive pressure assessment and animals were then terminated, and their hearts harvested for structural and molecular analyses.

Study 2 was performed to assess LV and RV wet and dry lung weights, as well as RV and LV water content, as previously described [20]. Briefly, animals underwent PAB as described in study 1, followed by randomisation to vehicle or dapagliflozin, 0.5mg BID by oral gavage. Six weeks later, animals were terminated, and their hearts/lungs harvested wet/dry weights.

Assessment of Cardiac Function

Echocardiography

Transthoracic echocardiography was performed in lightly anaesthetized rats with Isoflurane (1-1.5% mixed with 1 L/min 100% O_2) using the Vevo 2100 system (MS-250 transducer, Visualsonics, Toronto, ON). Briefly, the rats were placed on a pad equipped with a built-in electronically controlled heater and ECG electrodes (THM150, Indus Instruments, Webster, TX) to monitor ECG, body temperature and respiration during imaging. The mitral inflow peak velocities (E- and A-waves) and tricuspid annular plane systolic excursion (TAPSE) recordings were made from the apical four chambers view. Right ventricular thickness, fractional shortening (FS), stroke volume (SV), heart rate (HR) and cardiac output (CO) measurements were obtained by m-mode imaging in the parasternal long- and short-axis views. Images were acquired and analyzed offline (Vevo 2100 software v. 1.8) by a single investigator in a blinded manner.

Hemodynamic measurements

In a terminal experiment, RV hemodynamics were measured immediately following echocardiography. A 2F conductance catheter (Millar Instruments, Inc, Houston, Tx) was inserted into the RV through the apex, as previously described[19,21,22]. The maximal rates of ventricular pressure rise and fall (dp/dt_{max}, dp/dt_{min}) were calculated as indices of systolic and diastolic function. Ventricular relaxation was reflected by Tau- the time constant of mono-exponential decay of ventricular pressure during isovolumic relaxation. Load-independent measures of contractility and relaxation were reflected by the end-systolic and end-diastolic pressure-volume relationship (ESPVR and EDPVR, respectively) determined from a family of pressure-volume loops recorded during transient occlusion of the inferior vena cava. Stroke volume measured by echocardiography was used to calibrate the catheter-derived conductance signal, as previously described[23].

Histology

A 5-mm slice of the heart was cross-cut. Tissue was immersion-fixed in 4% paraformaldehyde buffer (pH 7.0) for at least 24-hours; dehydrated in graded ethanol and left overnight in xylene. After paraffin

embedding, 4-µm sections were microtome-sectioned (Leica Microsystems A/S, Herlev, Denmark). RV and LV cross sectional area was analyzed as previously reported [21].

Collagen content

Cross-sectional samples of the LV and RV were obtained and fixed in 10% formalin, and paraffin blocks were cut into 4 mm sections, mounted on slides, and dried at 35 °C for 24-48 hours in preparation for microscopy as previously described (21). Percent collagen fibrosis was determined using immunohistochemistry for collagen type 1, and ten images per animal were obtained at 400 x magnification. The Halo image analysis platform (Indica Labs, Albuquerque, NM, USA) was used to quantify the percent of collagen type I, using methods described previously (16).

Immunoblotting

Immunoblotting of right ventricular homogenates was performed with the following antibodies SERCA2a 1:1000 (IID8F6) 1:1000,[1] phosphorylated- AMP activated protein kinase a (Thr172) (phospho-AMPK) 1:1000 (#2531, Cell Signaling Technology, Danvers, MA), LC3A/B (LC3) 1:1000 (#12741, Cell Signaling Technology) and GAPDH 1:1000 (#2118, Cell Signaling Technology). Densitometry was performed using Image J version 1.39 (National Institutes of Health, Bethesda, MD)[24].

Statistical Analysis

Descriptive statistics were reported as mean ± standard error of the mean (SEM). Overall, the groups were compared using a one-way ANOVA or test as appropriate for the sham and PAB groups, and each of the drug conditions (vehicle, dapagliflozin [DAPA]). Group comparisons were performed using one way ANOVA with Fisher LSD to correct for multiple comparisons. Statistical analyses were done on GraphPad Prism software (version 8.4.0, San Diego, CA, USA). A p-value < 0.05 was considered statistically significant.

Results

PAB animals develop RV hypertrophy

To determine whether PAB model induced RVH, we examined RV mass indexed to body weight and tibial length. The PAB animals that were administered vehicle demonstrated significantly lower body weight, but higher RV weight indexed to tibial length, with no change in LV weight or lung weight indexed to tibial length when compared to sham + vehicle animals (**Table 1**). PAB + dapagliflozin significantly reduced RV weight indexed to tibial length when compared to PAB + vehicle. There was no change in lung weight or LV weight in PAB + dapagliflozin treated animals when compared to PAB + vehicle. Sham animals treated with dapagliflozin demonstrated a reduction in body weight and increased kidney weight indexed to tibial length when compared to sham + vehicle ($p<0.05$, **Table 1**).

Tables 1: Animal characteristics

	Sham + vehicle	Sham + dapagliflozin	PAB + vehicle	PAB + dapagliflozin
Body weight	284 ± 12	262 ± 20	265± 17	253 ± 13*
Urine Output (ml/24h)	10.5 ± 3.1	27.4 ± 4.8*	8.8 ± 1.9	27 ± 3.8*†
Urine Sodium (ml/24h)	85.9 ± 28	143 ± 47*	148 ± 33*	113 ± 46*†
Urine glucose (ml/24h)	1.7 ± 2.3	592 ± 120*	4.8 ± 2.1	511± 90*†
HbA1c (%)	4.5 ± 0.2	4.6 ± 0.2	4.5 ± 0.3	4.3 ± 0.2
Blood glucose (mmol/L)	12.7 ± 1.6	9.8 ± 1.4*	12.1 ± 3	11.3 ± 3.9
Hematocrit (%)	47.1 ± 0.4	47.2 ± 0.5*	46 ± 0.4	46.5 ± 0.6
Hemoglobin (g/L)	151 ± 2.2	156 ± 4.8	150 ± 5	153 ± 5.1
Systemic BP (mmHg)	111 ± 9	116 ± 11	112 ± 8	116 ± 8
Kidney Weight indexed to tibial length (g/mm)	39.5 ± 1.4	43.1 ± 2.7*	38.3 ± 23	40.2 ± 2.4†
Lung Weight indexed to tibial length (g/mm)	7.3 ± 0.8	6.8 ± 1.2	7 ± 0.9	6.7 ± 0.5*
Left ventricle Weight indexed to tibial length (g/mm)	13.7 ± 0.5	13.3 ± 1.3	13.3 ± 0.9	12.8 ± 0.7*
Right ventricle Weight indexed to tibial length (g/mm)	3.4 ± 0.3	3.2± 0.4	7.2 ± 1.7*	5.9± 1.9*†

Data are mean ± standard error of the mean. N=22 for each of sham + vehicle and sham + dapagliflozin. N=30 for PAB + vehicle and n=29 for PAB+ dapagliflozin. *= $p<0.05$ when c/w sham + vehicle † = $p<0.05$ when c/w PAB + vehicle

Dapagliflozin causes osmotic diuresis

Sham animals treated with dapagliflozin demonstrated a significant increase in urinary output, urinary sodium and glucose when compared to vehicle sham animals. Further, sham + dapagliflozin treated animals demonstrated a significant increase in hematocrit (all $p<0.05$, **Table 1**). PAB + dapagliflozin increased urinary output and urinary glucose, when compared to PAB + vehicle but was associated with a reduction in urinary sodium content. PAB + dapagliflozin did not alter either hematocrit or hemoglobin when compared to PAB+ vehicle of sham animals (p=NS, **Table 1**). HbA1c was not different across any group.

Effects of dapagliflozin on echocardiographic findings

Systemic BP was not different across any group. PAB + dapagliflozin treated animals demonstrated a reduction in HR when compared to sham and PAB+ vehicle. There was no change in LV systolic function

across any group. LV diastolic function, as measured by the Mitral inflow E to A ratio, was reduced in the PAB + vehicle animals when compared to sham. There was a trend towards normalising LV diastolic function with PAB + dapagliflozin (p=0.12). Cardiac output was reduced in PAB + dapagliflozin animals when compared to sham + vehicle. RV function, as assessed by RV fractional area change was not different between PAB + vehicle animals when compared to PAB + dapagliflozin. PAB + vehicle animals demonstrated a significant increase in RV wall thickness (p<0.05, Table 2), which was not altered by dapagliflozin treatment.

Table 2
Echocardiographic parameters

	Sham + vehicle	Sham + dapagliflozin	PAB + vehicle	PAB + dapagliflozin
Heart rate (BPM)	374 ± 41	370 ± 44	356 ± 35	328 ± 27*†
Cardiac output (ml/min)	80 ± 16	78 ± 21	76 ± 16	67 ± 11*
LV Fractional shortening (%)	54 ± 9	59 ± 8	55 ± 9	52 ± 10
Mitral valve E velocity (mm/s)	970 ± 140	929 ± 150	906 ± 97	825 ± 120*
Mitral valve A velocity (mm/s)	426 ± 130	449 ± 88	491 ± 87	400 ± 91†
Mitral E/A ratio	2.5 ± 0.2	2.1 ±0.1	1.9 ± 0.08 *	2.1 ±0.1
RV thickness; diastole (mm)	0.62 ± 0.13	0.61 ± 0.11	1.14 ± 0.26*	1.04 ± 0.2*

Data are mean ± standard error of the mean. N=22 for each of sham + vehicle and sham + dapagliflozin. N=30 for PAB + vehicle and n=29 for PAB+ dapagliflozin *= p<0.05 when c/w sham + vehicle † = p<0.05 when c/w PAB + vehicle

Impact of PAB + dapagliflozin upon invasive hemodynamics

Assessment of right ventricular (RV) function using invasive hemodynamics demonstrated that PAB animals had a significant increase in RV end systolic pressure (RVESP), dP/dt max and min, PRSW and ESPVR when compared to sham animals (all p<0.01, **Table 3**). The RV ESP was <50% of systemic pressure suggesting modest pulmonary hypertension. There was no change in RV end diastolic pressure with PAB (p=NS). PAB + dapagliflozin, when compared to PAB + vehicle did not affect RVESP, RVEDP or load sensitive (+dPdt max) or insensitive measures of systolic or diastolic function, (-dPdt max, ESPVR, PRSW or EDPVR respectively, table 3, Figure 1).

Tables 3: RV Invasive parameters

	Sham + vehicle	Sham + dapagliflozin	PAB + vehicle	PAB + dapagliflozin
RV end systolic pressure (mmHg)	19 ± 1	15 ± 2	41 ± 3*‡	46 ± 3*‡
RV end diastolic pressure (mmHg)	3.5± 0.2	3.5± 0.3	4.2± 0.3	4.6± 0.4
RV dpdt max (mmHg/s)	1259 ± 74	1360 ± 88	2160 ± 105*‡	2188 ± 103*‡
RV dpdt min (mmHg/s)	-788 ± 35	-744 ± 56	-1288 ± 90*‡	-1483 ± 98*‡
Tau (msec)	17 ± 1	19 ± 1	16 ± 1	18± 1
RV End systolic pressure volume relationship (AU)	131 ± 13	116 ± 22	341 ± 26*‡	301 ± 32*‡
RV End diastolic pressure volume relationship (AU)	8 ± 2	6 ± 1	17 ± 1*‡	15 ± 2*‡
Preload recruitable stroke work index (mmHg/SW)	19 ± 1	16.8 ± 2	40 ± 3*‡	41 ± 3*‡
TAPSE (mm)	2.2 ± 0.1	2.2 ± 0.1	1.8 ± 0.1*‡	1.7 ± 0.1*‡

Data are mean ± standard error of the mean. AU= arbitrary units. N=22 for each of sham + vehicle and sham + dapagliflozin. N=30 for PAB + vehicle and n=29 for PAB+ dapagliflozin

*= $p<0.001$ when c/w sham + vehicle † = $p<0.001$ when c/w PAB + vehicle, ‡ = $p<0.001$ when c/w sham + dapagliflozin

Dapagliflozin did not impact RV or LV fibrosis or cardiomyocyte size

To assess the effects of the PAB on extracellular matrix remodeling, we examined cardiomyocyte size, and type I collagen. We found that type I collagen was significantly increased in both the LV and RV of animals who underwent PAB when compared to sham + vehicle. Treatment with dapagliflozin in PAB animals had no effect upon Collagen I in either RV or LV. Myocyte size, measured in both the RV and LV was not impacted by dapagliflozin in either sham or PAB animals (Figure 2 and 3).

Impact of dapagliflozin upon SERCA2A, AMPK, and LC3-I/II

PAB + vehicle animals demonstrated a significant reduction in protein content of the calcium handling protein, SERCA2A ATPase, when compared to sham + vehicle animals. Furthermore, PAB reduced adenosine monophosphate-activated protein kinase (AMPK) protein expression, and the autophagy marker LC3B I/II ratio (all $p<0.05$ when c/w sham + vehicle). SERCA, AMPK and LC3BI/II expression was normalized by dapagliflozin treatment in PAB animals ($p<0.05$, Figure 4).

Study 2: Impact on RV/LV weight and dry weight as well as water content.

Given that PAB + dapagliflozin animals showed a reduction in RVH, without a change in myocyte size when compared to PAB + vehicle, we hypothesized that the reduction in RV mass may be mediated by a change in ventricular water content, either intra or extracellular.

As expected, PAB + vehicle treated animals demonstrated a significant increase in both wet and dry LV and RV weights when compared to sham (Table 4, **both p<0.05)**. Dapagliflozin treatment reduced both LV and RV water content (Table 4, **both p<0.05)**. However, when RV dry weight was indexed to tibial length, there was a non-significant trend towards a difference seen between PAB+ dapagliflozin versus PAB + vehicle treated animals (p=0.06), suggesting that the reduction in RV mass was predominated mediated by altered tissue water content, as opposed to a reduction in excess sarcomeres induced by PAB per se.

Table 4

	Sham + vehicle	Sham + dapagliflozin	PAB + vehicle	PAB + dapagliflozin
LV wet weight (g)	515 ± 9	481 ± 8*	498 ± 9*	477 ± 9*
LV dry weight (g)	126 ± 2	118 ± 2*	117 ± 3*	115 ± 2*
RV wet weight (g)	147 ± 4	138 ± 4*	314 ± 9*	276 ± 18*†
RV dry weight (g)	34 ± 1	33 ± 1*	70 ± 2*	64 ± 4*†
LV water content (%)	75.6 ± 0.1	75.5 ± 0.1	76.5 ± 0.1*	75.9 ± 0.1*
RV water content (%)	76.5 ± 0.2	76.0 ± 0.1	77.6 ± 0.1*	76.8 ± 0.2*†‡
LV wet weight indexed to TL (g/mm)	3.7 ± 0.1	3.5 ± 0.1	8.0 ± 0.2*	7.1 ± 0.5*†‡
RV wet weight indexed to TL (g/mm)	0.88 ± 0.02	0.85 ± 0.02	1.8 ± 0.5*‡	1.6 ± 0.1*‡
Data are mean ± standard error of the mean. N=11 for each of sham + vehicle and sham + dapagliflozin. N=9 for PAB + vehicle and n=7 for PAB+ dapagliflozin				
*= p<0.001 when c/w sham + vehicle † = p<0.001 when c/w PAB + vehicle, ‡ = p<0.001 when c/w sham + dapagliflozin				

Discussion

Despite intense interest, the exact mechanisms by which SGLT2 inhibition provides cardiac protection remains unclear. Herein we demonstrate that despite RV hypertension, the SGLT2i dapagliflozin

1. reduced RV mass

2. reduced RV and LV water content
3. improved proteins involved in nutrient sensing, contractility, and cellular homeostasis in a model of stable, compensated RV hypertrophy induced by pulmonary artery banding.

These findings suggest that a possible primary mechanism of cardiac protection involves the osmotic diuresis and reduced intra/extracellular water content, with secondary beneficial effects upon important molecular remodeling parameters.

With multiple therapies now available to treat left ventricular remodeling[5], attention has focused upon the RV. Importantly, RVH is an independent predictor of outcomes in a range of diseases [3]. Like the LV, in response to a pathologic stimulus the RV undergoes a robust remodeling response, characterized by alterations in matrix and cellular composition, resulting ultimately in RV fibrosis, RV hypertrophy, along with changes in metabolism and function[7]. However, unlike the LV, therapies such as renin angiotensin system inhibition (RASi), which have been associated with the prevention of LVH and HF[25] demonstrate different responses in the RV and RAS activation (and inhibition) is not as efficient in inducing or protecting against RVF. As a result, novel therapies are needed to address this limitation.

SGLT2i offer promise in this regard, being shown to improve renal and incident and prevalent HF outcomes, with a variety of mechanisms proposed. We have previously shown that the SGLT2i empagliflozin, when compared to “standard of care” reduced LV mass in persons with type 2 diabetes and established atherosclerotic disease, with the effect upon LV mass being independent upon changes in blood pressure[17]. Furthermore, we recently assessed extracellular volume (ECV) fraction in a sub study of the EMPA HEART study[16]. We showed that empagliflozin, reduced ECV, with a trend towards reducing intracellular volume fraction or iICV. These findings suggest that part of the direct effect of SGLT2i *in vivo* upon LV mass regression is mediated by changes in extracellular, and possibly intracellular water content. In the current study, we showed that LV water content was increased in PAB + vehicle animals when compared to sham + vehicle, and that dapagliflozin reduced LV water content, thus supporting our human studies.

As it relates to the RV, experimental data using the monocrotaline model of pulmonary hypertension has demonstrated a direct impact of the SGLT2i empagliflozin upon right ventricular hypertrophy[26]. However, the aforementioned study did not assess whether the reduction in RV mass was due to a change in myocyte size and mass, or whether it was related to changes in intra and extracellular volume fraction and water content.

Using the highly selective SGLT2i dapagliflozin, we observed two findings. The first was a reduction in RVH independent of changes in blood pressure, however the reduction in RV mass was primarily driven by a reduction in water content, as opposed to changes in myocyte hypertrophy assessed by cross sectional area. Secondly, these changes were associated with normalization of key proteins involved in nutrient sensing, contractility, and cellular homeostasis, such as AMPKinase. Furthermore, in keeping with our previous studies in non-diabetic models assessing LV remodeling[27], we did not see a reduction in

collagen type I in dapagliflozin treated PAB animals. The reduction in water content in the RV parallels the LV finding seen in the EMPA HEART LV ECV sub study. How this translates into the global prevention and treatment of RVF unfortunately remains unclear.

Postulated mechanisms for the change in RV and LV water content include the osmotic diuresis caused by SGLT2i, demonstrated by the increase in urinary sodium and glucose. We have previously demonstrated that SGLT2i results in an early natriuresis[18], but longer therapy likely results in compensatory distal tubule sodium reabsorption, ameliorating the natriuresis instead promoting osmotic diuresis. Other mechanisms to account for the cardioprotective properties of SGLT2i involve improved myocardial energetics because of either altered substrate delivery[28]. Here we demonstrate that the protein expression of the energy sensor AMPK was reduced by PAB and normalised by dapagliflozin. This finding extends the observations of Hawley et al which demonstrated that the SGLT2i canagliflozin, but not dapagliflozin or empagliflozin improved AMPK activity in HEK-293 cells, mouse embryonic fibroblasts as well as mice hepatocytes[29]. The “thrifty substrate” hypothesis has been suggested to account in part for the protective effects of SGLT2i. Whilst we did not assess for metabolism markers in the current study, previous work by our group has failed to demonstrate significant changes in gene expression in a non-diabetic rodent model of HFpEF, despite SGLT2i improving cardiac function and normalizing LV mass, supporting the concept that metabolic changes may be a secondary effect of SGLT2i and not the primary mode of action of the drug to improve cardiac outcomes. Packer has recently suggested that glucose lowering drugs may impact autophagy secondary to changes in AMPK and sirtuin activity[30]. Of note, our study identified a reduction in the LC3B I/II ratio, which was prevented by dapagliflozin therapy. The impact of improved energy biosensing and autophagic flux along with a reduction in oxidative stress is suggested to restore mitochondrial homeostasis and prevent myocardial dysfunction and the development of pathological RVH. Whilst the current study did not assess mitochondrial function, the improved energy biosensing and autophagic flux in a non-diabetic model with RVH, as opposed to the diabetic heart[30] suggests this may be a common mechanism to explain the beneficial effects of SGLT2i regardless of diabetic status.

Abnormal calcium handling is a hallmark of ventricular remodeling, with downregulation of proteins involved in calcium handling, such as the Sarcoplasmic calcium uptake ATPASE, SERCA 2A. Here in we found that PAB reduced SERCA 2A protein content. Treatment with dapagliflozin improved SERCA 2A content. Improved SERCA levels is associated with improved cardiac function and remains a novel finding. The mechanisms leading to normal SERCA 2A expression remain unclear and require further investigation, but our data supports the concept that SGLT2i prevents the downregulation of SERCA, as opposed to directly modifying transcriptional activity and increasing protein expression of SERCA.

Limitations

Our study was not without limitations. First, our PAB model recapitulated some, but not all aspects of RV remodeling and animals were in the compensated phase of remodeling, as evidence by preserved cardiac function and RV pressures being <2/3 systemic pressures. However, type 2 PH, the commonest cause of

PH typically demonstrates only modest elevations of RVESP, thus making the finding of reduced RV mass with dapagliflozin potentially more clinically relevant. Secondly, dapagliflozin was initiated soon after PAB, but the effects of SGLT2 inhibitors on cardiac remodeling may differ depending on timing of administration. Additional studies where these drugs are initiated at different times during the remodeling process will help to better understand whether the cardiac features can be altered late after the onset of RVF. Thirdly, SGLT2i has been shown to increase hematocrit secondary to increased erythropoietin production[31], which may result in improved oxygen delivery. We did not observe a change in Hct or Hb levels, suggesting that this is not the mediator of the mechanisms behind RV mass regression in PAB. Whether the lack of change in Hct in response to PAB or dapagliflozin impacts the relevance of these findings in humans and other models is unknown.

Finally, the exact mechanisms by which dapagliflozin reduced RVH remains unclear. We have previously shown that empagliflozin reduced ECV in persons with T2DM and ASCVD[16], which accounted for part of the reduction in LV mass observed in the EMPA HEART trial[17]. Whether the same impact was observed in the RV was unable to be assessed in that study. Further studies using CMR[32] focusing on the RV to assess ECV and cardiomyocyte compartments[33,34] is required to better understand the observed reduction in RVH, in persons both with, and without type 2 DM.

In conclusion, the SGLT2 inhibitor, dapagliflozin caused an osmotic diuresis and reduction in RV mass without significant changes in blood pressure, along with improvements in key nutrient, autophagic and contractility proteins within the RV, at an early compensated phase of RV remodeling. These finding suggest dapagliflozin may have a benefit for disease characterized by RVH induced by RV pressure loading.

Declarations

Ethics approval and consent to participate

The study design and protocol were reviewed and approved by the St. Michael's Hospital Animal care committee.

Consent for publication

Not applicable

Availability of data and materials

All data generated or analysed during this study are included in this published article.

Competing interests (disclosures)

Authors' contributions

KAC and REG designed study, and wrote manuscript. EW, AV, SNB, VGY, KT, LN, YZ, GK, JFD performed all experimental work and generated results. MFK and AA critically reviewed manuscript and made suggestions to results and discussion. All authors read and approved the final manuscript.

Acknowledgements:

We would like to thank the imaging facility core at SMH hospital.

Competing interests:

- KAC has received research grants to his institution from Astra Zeneca and Boehringer Ingelheim, received support for travel to scientific meeting from Boehringer Ingelheim and honoraria for speaking engagements and ad hoc participation in advisory boards from Astra Zeneca, Boehringer Ingelheim and Janssen. REG has received research grants to his institution from Astra Zeneca and Boehringer Ingelheim, received support for travel to scientific meeting from Astra Zeneca and honoraria for speaking engagements and ad hoc participation in advisory boards from Astra Zeneca, Boehringer Ingelheim and Janssen. A.A. has received research support through his institution from AstraZeneca and Boehringer Ingelheim and KC, REG and AA are listed as inventors on a patent application by Boehringer Ingelheim on the use of DPP-4 inhibitors in heart failure. All other authors declare that they have no competing interests

Funding

Studies were supported by research grants from the St. Michael's Hospital Foundation and Astra Zeneca. Dr. Gilbert is the Canada Research Chair in Diabetes Complication's, and this research was made possible, in part, by the Canada Research Chair's Program. A.A. is supported by a Diabetes Investigator Award from Diabetes Canada and holds the Keenan Chair in Medicine at St. Michael's Hospital and University of Toronto. V.G.Y. was supported by a Post-doctoral Fellowship from Diabetes Canada and is supported by a D H. Gales Family Charitable Foundation Post-doctoral Fellowship from the Banting and Best Diabetes Centre. Dr Kim A Connelly holds the Keenan chair for Research Leadership, at the Keenan Research centre for Biomedical Science, Toronto.

References

1. Friedberg MK, Reddy S. Right ventricular failure in congenital heart disease. Curr Opin Pediatr. 2019;31:604–10.

2. Gavazzoni M, Badano LP, Vizzardi E, Raddino R, Genovese D, Taramasso M, et al. Prognostic value of right ventricular free wall longitudinal strain in a large cohort of outpatients with left-side heart disease. European Hear J Cardiovasc Imaging. 2020;21:1013–21.

3. Geva T, Mulder B, Gauvreau K, Babu-Narayan SV, Wald R, Hickey K, et al. Preoperative Predictors of Death and Sustained Ventricular Tachycardia After Pulmonary Valve Replacement in Patients with

Repaired Tetralogy of Fallot Enrolled in the INDICATOR Cohort. Circulation. 2018;138:2106–15.

4. Surkova E, Muraru D, Genovese D, Aruta P, Palermo C, Badano LP. Relative Prognostic Importance of Left and Right Ventricular Ejection Fraction in Patients With Cardiac Diseases. J Am Soc Echocardiog. 2019;32:1407-1415.e3.

5. Burchfield JS, Xie M, Hill JA. Pathological Ventricular Remodeling. Circulation. 2013;128:388–400.

6. Xie M, Burchfield JS, Hill JA. Pathological Ventricular Remodeling: Therapies: Part 2 of 2. Circulation. 2013;128:1021–30.

7. Friedberg MK, Redington AN. Right Versus Left Ventricular Failure. Circulation. 2014;129:1033–44.

8. Ryan JJ, Archer SL. The Right Ventricle in Pulmonary Arterial Hypertension. Circ Res. 2014;115:176–88.

9. Roche SL, Redington AN. Right Ventricle. Circulation. 2013;127:314–6.

10. Roche SL, Redington AN. The Failing Right Ventricle in Congenital Heart Disease. Can J Cardiol. 2013;29:768–78.

11. Bogaard HJ, Natarajan R, Henderson SC, Long CS, Kraskauskas D, Smithson L, et al. Chronic Pulmonary Artery Pressure Elevation Is Insufficient to Explain Right Heart Failure. Circulation. 2009;120:1951–60.

12. Noordegraaf AV, Chin KM, Haddad F, Hassoun PM, Hemnes AR, Hopkins SR, et al. Pathophysiology of the right ventricle and of the pulmonary circulation in pulmonary hypertension: an update. Eur Respir J. 2019;53:1801900.

13. Vonk-Noordegraaf A, Haddad F, Chin KM, Forfia PR, Kawut SM, Lumens J, et al. Right Heart Adaptation to Pulmonary Arterial Hypertension. J Am Coll Cardiol. 2013;62:D22–33.

14. Wiviott SD, Raz I, Bonaca MP, Mosenzon O, Kato ET, Cahn A, et al. Dapagliflozin and Cardiovascular Outcomes in Type 2 Diabetes. New Engl J Med. 2019;380:347–57.

15. McMurray JJV, Solomon SD, Inzucchi SE, Køber L, Kosiborod MN, Martinez FA, et al. Dapagliflozin in Patients with Heart Failure and Reduced Ejection Fraction. New Engl J Med. 2019;381:1995–2008.

16. Mason T, Coelho-Filho OR, Verma S, Chowdhury B, Zuo F, Quan A, et al. Empagliflozin Reduces Myocardial Extracellular Volume in Patients With Type 2 Diabetes and Coronary Artery Disease. Jacc Cardiovasc Imaging. 2021;

17. Verma S, Mazer CD, Yan AT, Mason T, Garg V, Teoh H, et al. Effect of Empagliflozin on Left Ventricular Mass in Patients With Type 2 Diabetes Mellitus and Coronary Artery Disease. Circulation. 2019;140:1693–702.

18. Opingari E, Verma S, Connelly KA, Mazer CD, Teoh H, Quan A, et al. The impact of empagliflozin on kidney injury molecule-1: a subanalysis of the Effects of Empagliflozin on Cardiac Structure, Function, and Circulating Biomarkers in Patients with Type 2 Diabetes CardioLink-6 trial. Nephrol Dial Transpl. 2020;35:895–7.

19. Akazawa Y, Okumura K, Ishii R, Slorach C, Hui W, Ide H, et al. Pulmonary artery banding is a relevant model to study the right ventricular remodeling and dysfunction that occurs in pulmonary arterial hypertension. J Appl Physiol. 2020;129:238–46.

20. Chen Y, Guo H, Xu D, Xu X, Wang H, Hu X, et al. Left Ventricular Failure Produces Profound Lung Remodeling and Pulmonary Hypertension in Mice. Hypertension. 2012;59:1170–8.

21. Sun M, Ishii R, Okumura K, Krauszman A, Breitling S, Gomez O, et al. Experimental Right Ventricular Hypertension Induces Regional β1-Integrin–Mediated Transduction of Hypertrophic and Profibrotic Right and Left Ventricular Signaling. J Am Heart Assoc. 2018;7.

22. Ishii R, Okumura K, Akazawa Y, Malhi M, Ebata R, Sun M, et al. Heart Rate Reduction Improves Right Ventricular Function and Fibrosis in Pulmonary Hypertension. Am J Resp Cell Mol. 2020;63:843–55.

23. Borgdorff MAJ, Koop AMC, Bloks VW, Dickinson MG, Steendijk P, Sillje HHW, et al. Clinical symptoms of right ventricular failure in experimental chronic pressure load are associated with progressive diastolic dysfunction. J Mol Cell Cardiol. 2015;79:244–53.

24. Gramolini AO, Trivieri MG, Oudit GY, Kislinger T, Li W, Patel MM, et al. Cardiac-specific overexpression of sarcolipin in phospholamban null mice impairs myocyte function that is restored by phosphorylation. P Natl Acad Sci Usa. 2006;103:2446–51.

25. Dahlöf B, Devereux RB, Kjeldsen SE, Julius S, Beevers G, Faire U de, et al. Cardiovascular morbidity and mortality in the Losartan Intervention For Endpoint reduction in hypertension study (LIFE): a randomised trial against atenolol. Lancet. 2002;359:995–1003.

26. Chowdhury B, Luu AZ, Luu VZ, Kabir MG, Pan Y, Teoh H, et al. The SGLT2 inhibitor empagliflozin reduces mortality and prevents progression in experimental pulmonary hypertension. Biochem Bioph Res Co. 2020;524:50–6.

27. Connelly KA, Zhang Y, Visram A, Advani A, Batchu SN, Desjardins J-F, et al. Empagliflozin Improves Diastolic Function in a Nondiabetic Rodent Model of Heart Failure With Preserved Ejection Fraction. Jacc Basic Transl Sci. 2019;4:27–37.

28. Ferrannini E, Mark M, Mayoux E. CV Protection in the EMPA-REG OUTCOME Trial: A “Thrifty Substrate” Hypothesis. Diabetes Care. 2016;39:1108–14.

29. Hawley SA, Ford RJ, Smith BK, Gowans GJ, Mancini SJ, Pitt RD, et al. The Na + /Glucose Cotransporter Inhibitor Canagliflozin Activates AMPK by Inhibiting Mitochondrial Function and Increasing

Cellular AMP Levels. Diabetes. 2016;65:2784–94.

30. Packer M. Autophagy-dependent and -independent modulation of oxidative and organellar stress in the diabetic heart by glucose-lowering drugs. Cardiovasc Diabetol. 2020;19:62.

31. Mazer CD, Hare GMT, Connelly PW, Gilbert RE, Shehata N, Quan A, et al. Effect of Empagliflozin on Erythropoietin Levels, Iron Stores and Red Blood Cell Morphology in Patients with Type 2 Diabetes and Coronary Artery Disease. Circulation. 2019;141:704–7.

32. Coelho-Filho OR, Mitchell RN, Moreno H, Kwong R, Jerosch-Herold M. MRI based non-invasive detection of cardiomyocyte hypertrophy and cell-volume changes. J Cardiov Magn Reson. 2012;14:O10.

33. Yamamura K, Yuen D, Hickey EJ, He X, Chaturvedi RR, Friedberg MK, et al. Right ventricular fibrosis is associated with cardiac remodelling after pulmonary valve replacement. Heart. 2019;105:855.

34. Yamamura K, Yuen D, Hickey E, Chaturvedi R, Friedberg M, Wald R. HISTOLOGICAL QUANTIFICATION OF RIGHT VENTRICULAR MYOCARDIAL FIBROSIS AND ITS IMPACT ON RIGHT VENTRICULAR REVERSE REMODELING IN ADULT PATIENTS WITH REPAIRED TETRALOGY OF FALLOT. J Am Coll Cardiol. 2018;71:A555.

Figures

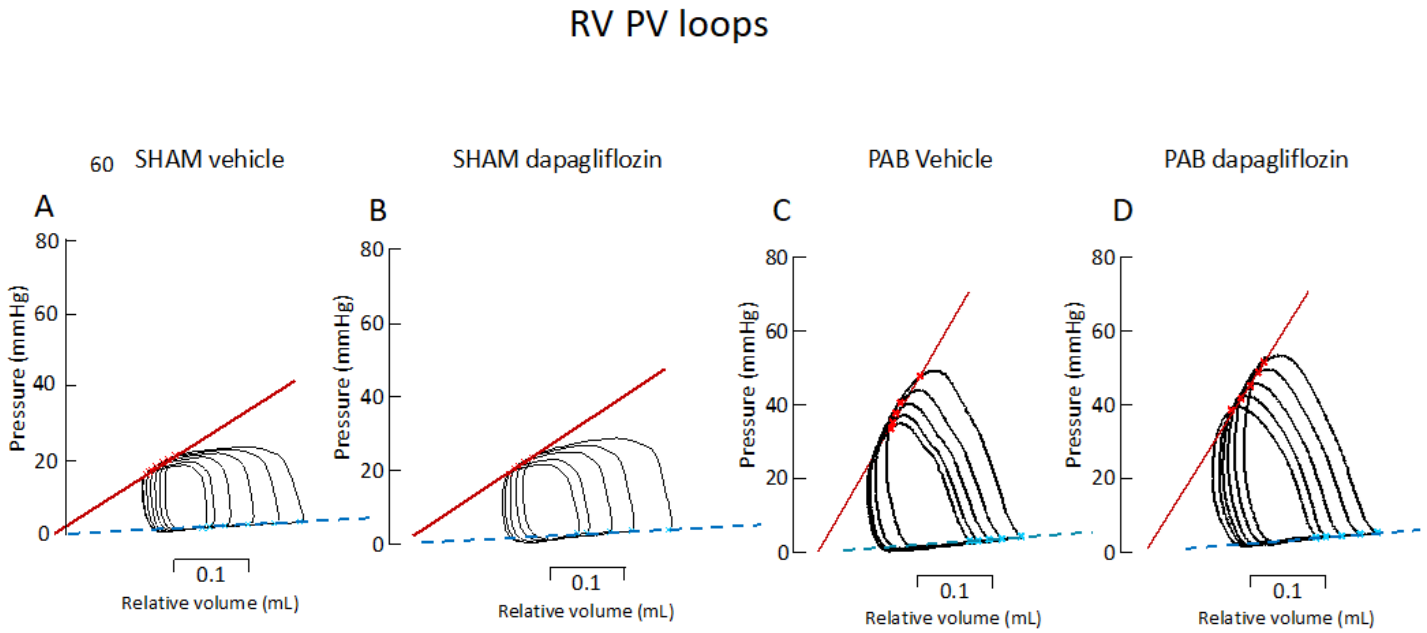

Figure 1

Right ventricular (RV)Pressure-volume (PV) analysis in rats. Representative RV PV loops in sham (A), pulmonary artery banding (PAB) vehicle treated (B) and PAB dapagliflozin treated rats (C). Stroke volume

measured by echocardiography was used to calibrate the catheter-derived conductance signal. ESPVR is represented by plain red lines, EDPVR by dashed blue lines.

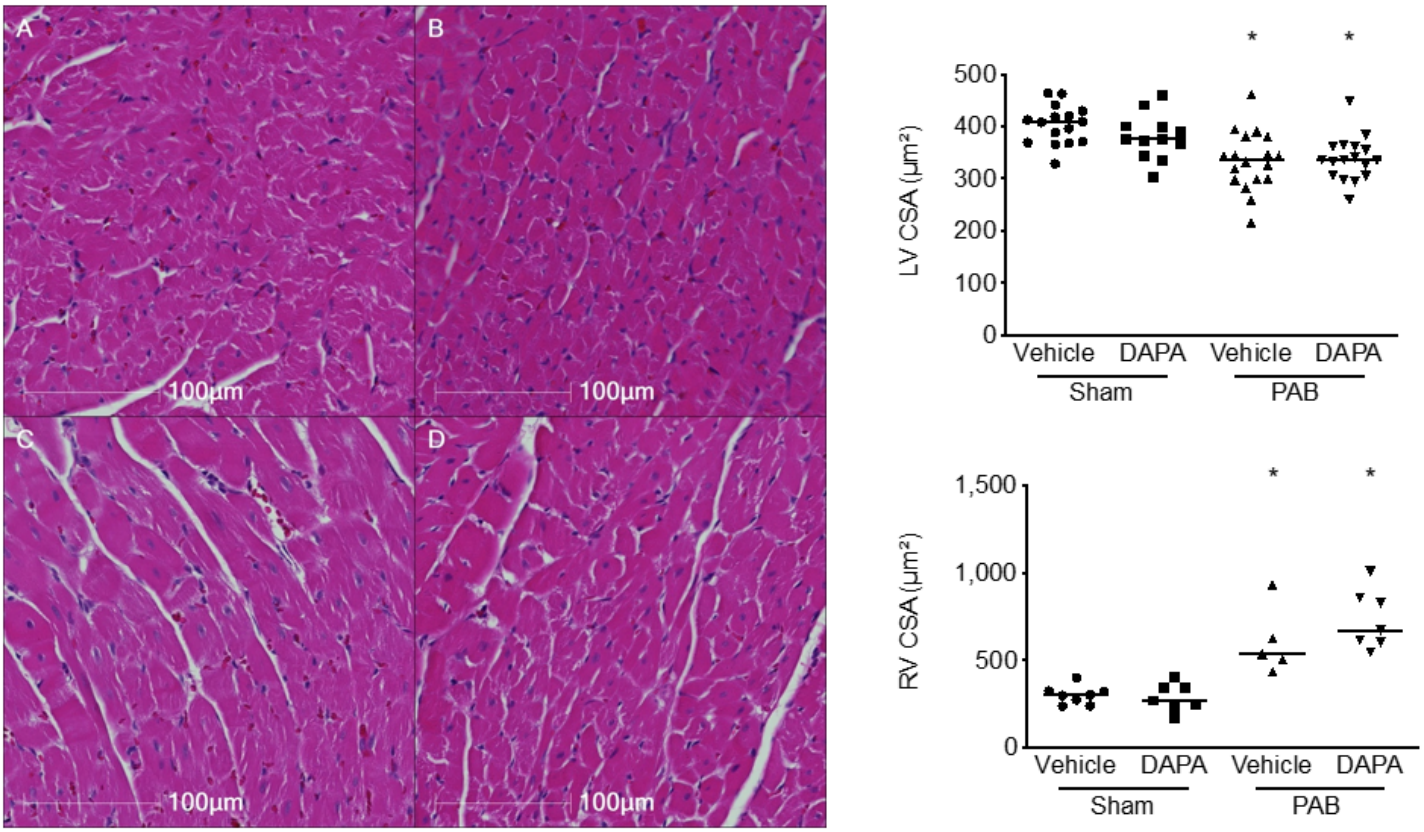

Representative images of H&E stained slides (LV).

Figure 2

Representative H+E staining to assess for cardiomyocyte cross sectional area of both LV and RV of sham + vehicle, sham + dapagliflozin, PAB + vehicle, PAB + dapagliflozin animals. Dapagliflozin did not impact cardiomyocyte CSA. Quantitative data on the right with LV upper right corner and RV lower right corner. *= $p<0.05$ when c/w sham + vehicle † = $p<0.05$ when c/w PAB + vehicle

Figure 3

Representative Collagen I immunostaining to assess for type 1 collagen of both LV and RV of sham + vehicle, sham + dapagliflozin, PAB + vehicle, PAB + dapagliflozin animals. PAB increased LV and RV collagen content. Dapagliflozin did not impact type 1 collagen expression. Quantitative data on the right with LV upper right corner and RV lower right corner. *= $p<0.05$ when c/w sham + vehicle

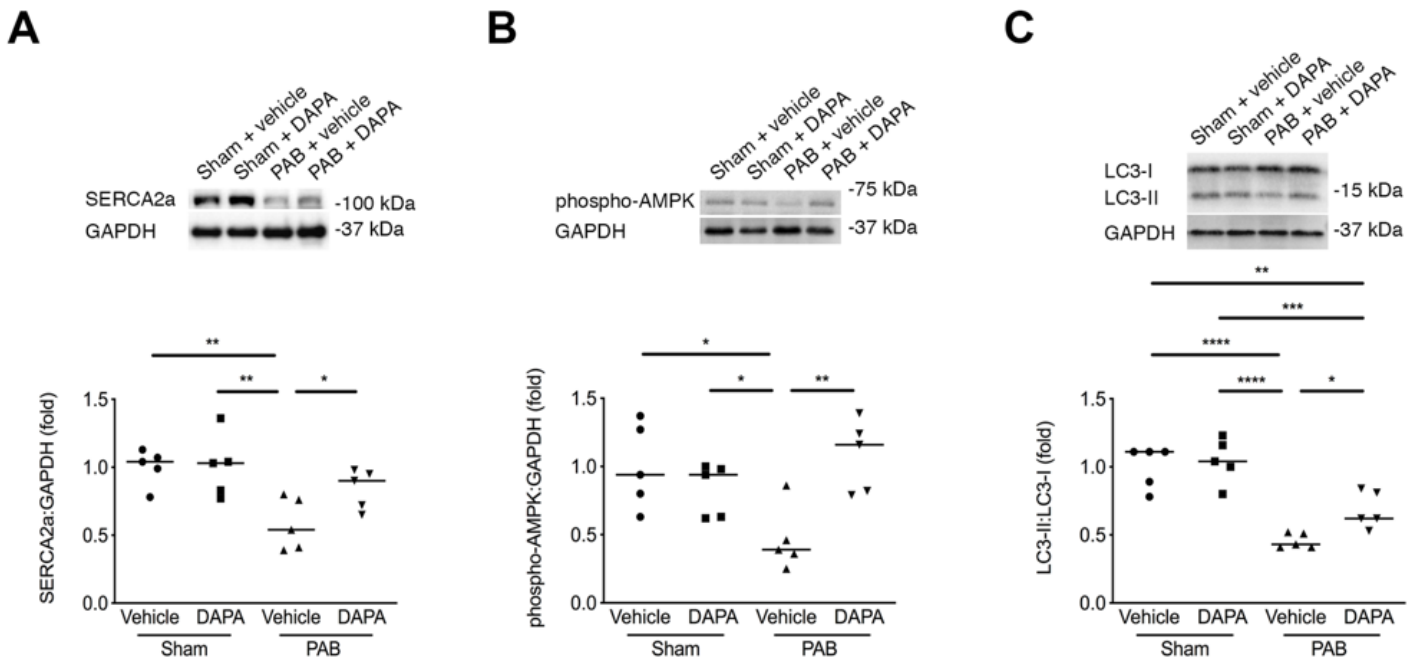

Figure 4

Decreased right ventricular SERCA2a, phospho-AMPK and LC3-II protein levels following pulmonary artery banding (PAB) are prevented by dapagliflozin (DAPA) treatment. Immunoblotting right ventricular homogenates from sham + vehicle, sham + DAPA, PAB + vehicle and PAB + DAPA (n=5/group) for SERCA2a (A), phospho-AMPK (B) or LC3-I/II. Values normalized to GAPDH for SERCA2a and phospho-AMPK or determined as the LC3-II:LC3-I ratio for LC3-I/II and shown as the fold change relative to sham + vehicle. *=p<0.05, **p=<0.01, ***p<0.001, ****p<0.0001 by one-way ANOVA followed by Fisher least significant differences post hoc test.